European Journal of Electrical Engineering and Computer Science
Vol 8 | Issue 3 | June 2024
ISSN 2736-5751

RESEARCH ARTICLE

Simulation and Dynamic Analysis of a Hybrid Renewable Power System for Postville, Labrador

Azadeh Farhadi and Muhammad Tariq Iqbal*

ABSTRACT

Recently, global energy and environmental challenges have been magnified by rising fuel consumption and greenhouse gas emissions. Remote areas without grid access face additional difficulties, driving the need for sustainable energy solutions. To address this pressing issue, a growing focus is on switching towards cleaner, renewable energy sources. This research attempts to tackle these challenges by implementing a dynamic model for Postville, an isolated location in Canada. The objective is to reduce costs and provide high-quality power output to meet the community's energy needs. The proposed hybrid renewable energy system (HRES) includes a 455 kW diesel generator, a 435 kW PV panel, five 100 kW wind turbines, a 306 kW power converter, and 720 batteries. Dynamic modeling and simulation using MATLAB-Simulink software are employed to evaluate the system's performance and dynamics under variable weather conditions. The simulation results demonstrate the system's reliability and ability to consistently deliver high-quality power output and meet the load demand.

Keywords: MPPT, Photovoltaic (PV), PID controller, Renewable energy.

Submitted: May 08, 2024

Published: June 24, 2024

10.24018/ejece.2024.8.3.628

Department of Electrical and Computer Engineering, Faculty of Engineering and Applied Science, Memorial University of Newfoundland (MUN), Canada.

Corresponding Author:
Email: tariq.mun@gmail.com

1. Introduction

Energy and the environment are expected to be two of the most significant and daunting global challenges of the 21st century. According to British Petroleum, fuel consumption in the past three decades has more than doubled, reaching 11,630,000 tonnes of oil equivalent (Mtoe) in 2009 [1]. As fuel consumption rises, there will be a corresponding increase in total greenhouse gas emissions and environmental impact. Therefore, it is necessary to offer alternative, cleaner energy sources like renewable energy. These renewable energy sources are free from pollution and have no environmental impact [2]. Currently, various renewable technologies are accessible, including photovoltaic (PV) or solar thermal, biomass, geothermal, wave, hydropower, and wind turbine (WT). However, among these options, PV and WT stand out as the most financially viable choices [3]. The primary drawback of both PV and WT systems is their seasonal variation in electricity generation: PV systems tend to produce more electricity in summer than in winter, whereas wind turbine systems typically yield higher outputs during winter [4]. Consequently, Hybrid Renewable Energy Systems (HRES), which integrate PV and wind turbines, are gaining more popularity, especially in remote areas. However, solar radiation and wind velocity fluctuations inevitably result in electricity production oscillations in such systems. Thus, appropriate electricity storage systems (ESS) are also necessary to address the intermittent nature of wind and solar energy [5]. Connecting HRES to storage options like batteries provides the capability to store surplus energy produced by solar and wind systems. This stored energy becomes valuable when insufficient sunlight or wind generates electricity. Consequently, HRES operates more effectively across all operational circumstances than individual renewable technologies [6]. In addition to the utilization of electricity storage systems, diesel generators can serve as backup power sources in remote areas where there is no access to the grid, ultimately enhancing efficiency and reliability [2]. Several studies have been conducted on dynamic analysis and design of renewable energy systems that use backup devices like energy storage systems and diesel generators.

Li *et al*. [7] simulated wind, solar, and backup devices like diesel generators as part of a hybrid power system for St. Lewis. They employed three different software tools to design this system. Their research indicates that approximately 86 per cent of electricity is supplied by wind and PV, which can significantly reduce greenhouse gas emissions.

Das and Akella [8] propose a power flow control system for photovoltaic, wind, and battery to tackle the issue

of fluctuating power generation from renewable sources. Using a fuzzy logic controller (FLC), the system balances power generation and load demand while maintaining the battery state of charge (SOC) within acceptable limits. Simulation results demonstrate effective power management, ensuring a stable supply and minimizing fluctuations. The FLC adjusts battery charging/discharging based on power generation, load demand, and SOC, while a dump load system absorbs excess power.

Koutrouli *et al*. [9] developed a genetic algorithm that optimized the dimensions of PV panels, wind turbines, and batteries in a system that can operate independently. As part of their study, they attempted to keep costs to a minimum while meeting load requirements without eliminating any loads. Based on simulation results, they demonstrated that Genetic algorithms for optimization were effective. Their approach addresses the critical need for cost-efficient and reliable power generation, particularly in remote or off-grid locations.

Belabbas *et al*. [10] innovatively applied genetic algorithms to refine the performance of a self-sufficient hybrid power system featuring PV panels, a diesel generator, and battery storage. Introducing a novel hierarchical power management scheme, they integrated fuzzy logic control mechanisms to meticulously uphold frequency and voltage at the prescribed coupling location, all while meticulously optimizing power extraction from the PV array. Their pioneering system boasted an impressive Total Harmonic Distortion of 5.9%.

Ceylan and Devrim [11] explore a hybrid renewable energy system for Turkish greenhouses, integrating PV panels, an electrolyzer, and a PEMFC. Surplus PV electricity is used for hydrogen production, stored for later use, and converted by PEMFCs into electricity and heat. Design factors include energy demand and component efficiency, with economic analysis emphasizing cost-effectiveness. The study underscores the potential of hybrid systems to meet energy needs efficiently and reduce environmental impact.

The paper's framework consists of the following sections: In Section 2, the case study is described, and Section 3 describes each proposed HRES component. Section 4 describes the simulation model for the HRES system. Control strategies, such as Maximum PowerPoint Tracking (MPPT), are examined in Section 5. Subsequently, Section 6 discusses the simulation outcomes. Section 7 contains the paper's summary.

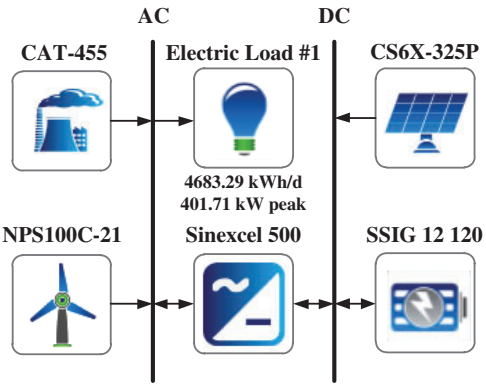

Fig. 1. Proposed hybrid power system schematic diagram [12].

TABLE I: PV Parameter

Technical data	Value
Maximum rated power	325 W
Cell per module	72
Maximum power voltage	37 V
Maximum power current	8.78 A
Temp coef of V_{oc}	−0.31%/°C
Temp coef of I_{sc}	0.053%/°C
Lifetime	25 years

TABLE II: WT Parameter

Technical data	Value
Rated power	100 kW
Rated voltage	400 V
Rated wind speed	15 m/s

TABLE III: Diesel Generator Parameter

Technical data	Value
Capacity	455 kW
Fuel type	Diesel
Rated voltage	208 to 600 V
Speed	1800 RPM

TABLE IV: Battery Parameter

Technical data	Value
Type	Lead-acid
Nominal voltage	12 V
Nominal capacity	1.42 kWh
Maximum capacity	118 Ah

2. Case Study

This research builds upon a previous study by the author, focusing on assessing the optimal size and economic feasibility of a hybrid power system designed for Postville [12]. The Postville community of Canada is located about 40 kilometers north of Kaipokok Bay. It is located in a remote area, so it does not have access to the power grid [12].

According to the findings in [12], Postville consumes over 500,000 liters of diesel per year from three diesel generators. Typical solar irradiation for the area is 2.87 kWh/m2/day, and an average annual wind speed of 7.81 m/s is measured at a 50 m height. Moreover, the average daily electrical demand is 401.71 kW, with a peak demand of 4683.2 kW.

In reference [12], it is mentioned that the most cost-effective and economical hybrid system configuration includes a PV, WT, DG, and battery. The schematic diagram illustrating this configuration is depicted in Fig. 1, and the technical details of the suggested setup are listed in Tables I–IV [12]. This setup comprises a 455 kW DG, a 435 kW PV panel, five 100 kW WT, and a 306 kW power converter. Notably, this system incurs minimal economic expenses, with a net present cost of $5,570,000. Additionally, this system consumes 77,245 liters of fuel annually.

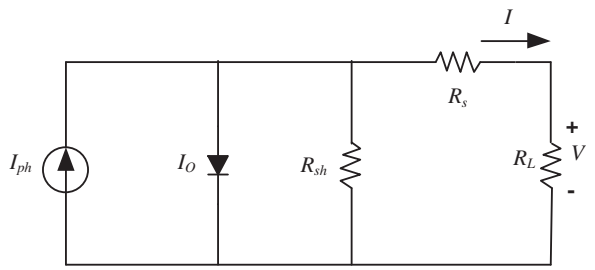

Fig. 2. Single-diode model equivalent circuit.

3. HRES's Key Elements Modeling

3.1. Photovoltaic Panel (PV)

PV energy systems use PV modules to generate DC electric power from solar radiation. String or PV arrays can be created using these modules in series or parallel configurations. It is essential to have an inverter to transform the PV system's DC output into AC power, ensuring that loads are supplied with electricity. PV systems are affected by solar radiation, temperature, and the type of cell they use to generate power [13].

Fig. 2 illustrates a single-diode scheme developed to represent the features and performance of a solar panel, considering energy losses. This model incorporates a series resistance (R_s) to signify energy dissipation encountered by current flowing through the cell body, wires, and conductive surfaces, along with a shunt resistance (R_{sh}) representing leakage current [14].

To draw the power-voltage characteristics (P-V) curve, Kirchhoff's current law is used to derive Eq. (1) [14].

$$I_{PV} = I_{ph} - I_d - I_{sh} \tag{1}$$

where I_{PV} represents the cell's output current, I_{ph} signifies the cell photocurrent, I_d refers to the current flowing through the diode, and I_{sh} represents shunt resistance leakage current (R_{sh}).

Furthermore, the current of a diode can be determined using Eq. (2) [15].

$$I_d = I_0 \left[exp \left[\frac{V_d}{V_{tv}} - 1 \right] \right] \tag{2}$$

where I_0 represents saturation current across the diode, V_d signifies diode voltage and V_{tv} is the thermal voltage equivalent. V_d are obtained by Eq. (3) [15].

$$V_d = V_{PV} + I_{PV} \times R_S$$

$$V_{tv} = \frac{KT}{q} \times A \times N_{cell} \tag{3}$$

where V_{PV} is PV output voltage, R_S is the series resistance, K is the Boltzmann constant, T stands for Kelvin temperature, q denotes a charge on an electron, A stands for the diode ideality value and N_{cell} indicates the number of series cells. Finally, I_{sh} can be calculated by Eq. (4) [15].

$$I_{sh} = \frac{V_{PV} + I_{PV} \times R_S}{R_{Sh}} \tag{4}$$

3.2. Wind Turbine

A wind energy setup consists of three parts. Air's kinetic energy is converted into rotational energy during the aerodynamic phase. Afterward, a wind turbine and gearbox adjust torque and speed before feeding them into the generator, where the energy of mechanical motion is converted to three-phase electricity waves. A third stage, known as Electrical, involves the control and transformation of electrical signals using inverters and converters to achieve various values of voltage [16]. The WT modeling stages are illustrated in Fig. 3.

The correlation between the speed of the wind and its energy in a WT can be formulated as [17].

$$P = \frac{1}{2}. \rho. A. Cp\ (\beta, \lambda). v^3 \tag{5}$$

Here, P represents the maximum power, ρ stands for the air density within the area covered by the turbine, Cp denotes the power coefficient obtained from Eq. (6), and v represents the wind speed [17].

$$C_p(\beta, \lambda) = c_1 \left(\frac{c_2}{z} - c_3\beta - c_4 \right) e^{\frac{-c5}{2}} + c_6^{\lambda} \tag{6}$$

where $c_1 = 0.5176$, $c_2 = 116$, $c_3 = 0.4$, $c_4 = 5$, $c_5 = 21$ and $c_6 = 0.0068$. β denotes the pitch angle for the blades, while λ represents the tip speed ratio that can be calculated by Eq. (7) [17].

$$\lambda = \frac{R\omega_{wt}}{v} \tag{7}$$

where R represents the turbine radius, ω_{wt} stands for the turbine speed, and v denotes the wind speed.

3.3. Diesel generator

A diesel generator operates by first utilizing diesel fuel to generate mechanical energy within its engine. This mechanical energy is then converted into electrical energy through a component known as the governor. The governor regulates the speed and output of the generator to ensure a steady supply of electricity. In essence, the diesel generator transforms the chemical energy stored in diesel fuel into usable electrical power through a series of mechanical and electrical processes. There are four main components of a DG setup: a governor, an engine, a synchronous generator, and excitation [18]. The mechanism regulates the engine velocity by correlating the fuel intake with the flywheel speed, accounting for engine inertia's intricate dynamic impacts. The engine transforms the fuel flow ∅ into mechanical torque T_{tq} following a delay period t_1 governed by an engine torque constant C_1. The equation governing the mechanical motion is as follows [19]:

$$T_{tq} = C_1 e^{-t_1 s} \varnothing(s) \tag{8}$$

In this study, a diesel generator serves as a backup power source when there is insufficient power from the PV panels and battery system.

3.4. Energy Storage

Lead-acid batteries are the main storage component in PV systems. This component is primarily responsible for

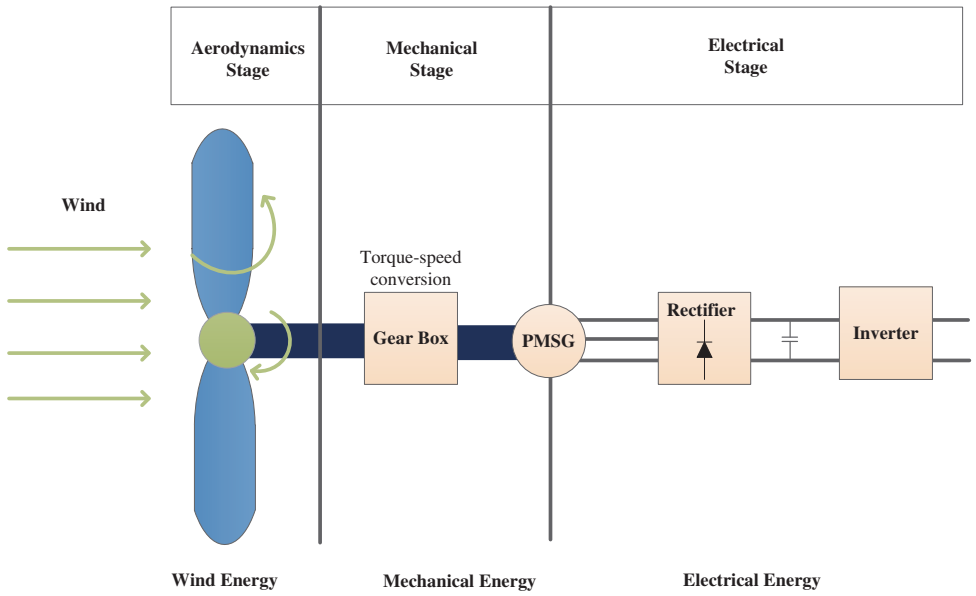

Fig. 3. Wind turbine electrical system.

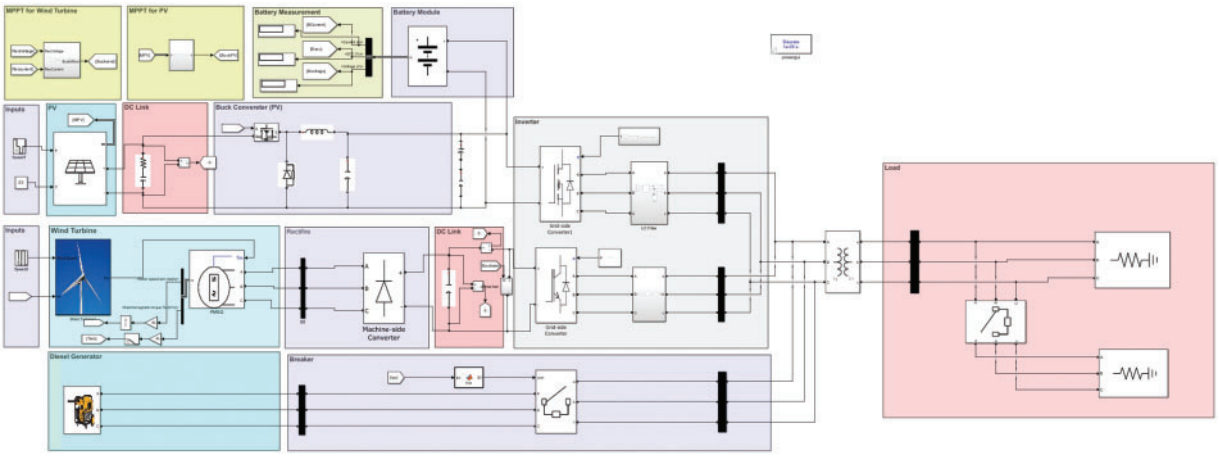

Fig. 4. MATLAB simulation model for proposed hybrid power systems.

storing and transferring energy within a PV system. It is possible to convert stored chemical energy from chemical to electrical and vice versa. A battery's behavior is generally described by its voltage as shown in Eq. (9) [20].

$$V_{Es} = V_{OC} \pm IR \tag{9}$$

The open circuit voltage is V_{OC}, and the internal resistance is R. The current I is positive during charging and negative during discharging. The internal resistance fluctuates and relies on various factors such as capacity, current flow during charging or discharging, temperature, and other parameters.

4. HRES's System Simulation Model

The model utilized to simulate the proposed hybrid renewable energy system (HRES) is depicted in Fig. 4. Each component is explained in detail as follows.

4.1. PV System and Battery Storage

The PV array comprises 15 photovoltaic modules linked in series and 90 modules linked in parallel, with an individual power rating of 325 watts. Power curves and a detailed I–V curve produced by the PV modules are depicted in Fig. 5. The PV system's output is linked to an 1100 μF and 0.001 Ω DC link capacitor and resistor.

In the proposed system the PV utilizes a buck converter to reduce voltage levels. The MOSFET of the buck converter is governed by an MPPT algorithm, with initial parameters including D_{max} and D_{min}, set to 0.95 and 0, respectively, where D referring the duty cycle. A buck converter is linked to a lead-acid battery with a rated capacity of 2832 Ah.

A fully bridged three-phase inverter employing IGBT technology is linked to an LC filter and the filter is connected to a transformer with three phases. The DC-AC inverter functions at a frequency of 60 Hz, featuring an input voltage of 360 V and an output root mean square (RMS) voltage of 360 V. The LC filter has widespread application at the output of PWM inverters, especially when voltage control is the primary objective. The provided filter has been configured to operate at a switching frequency of 10 kHz, featuring an inductance of $Lf = 0.22918\ mH$ and a capacitance of $Cf = 0.92104\ mF$.

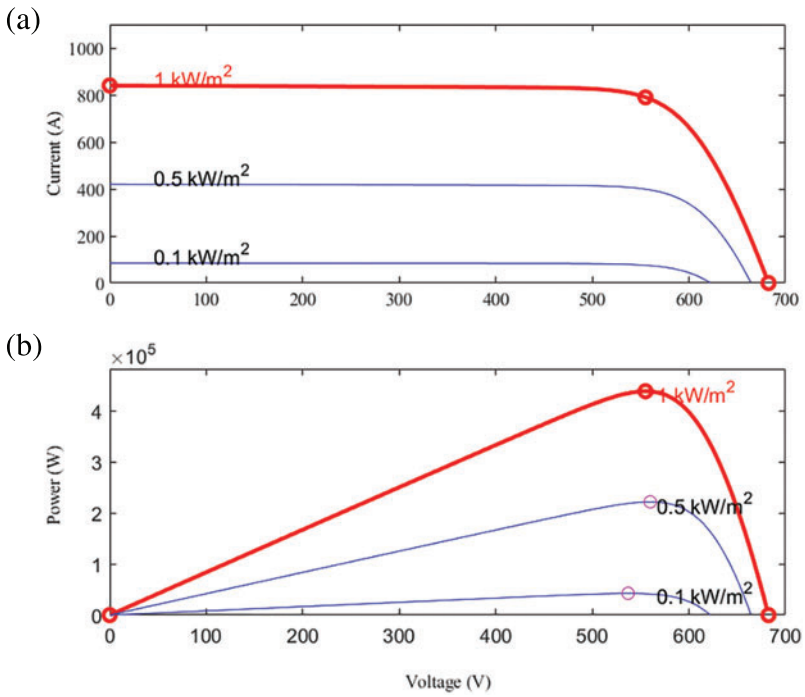

Fig. 5. PV output (a) current and (b) power under different irradiances.

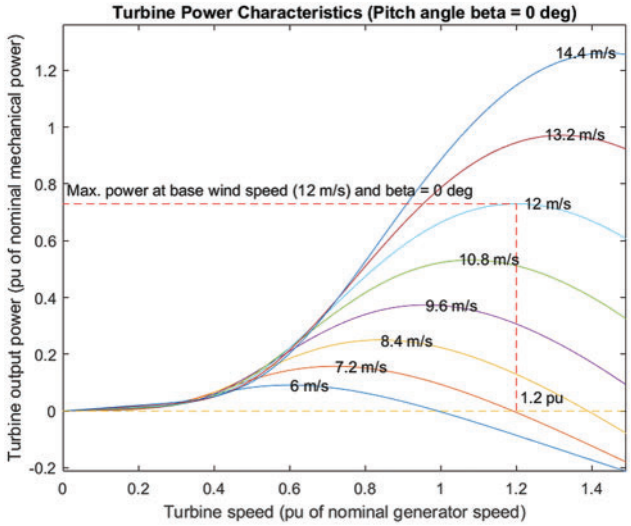

Fig. 6. Turbine power specifications.

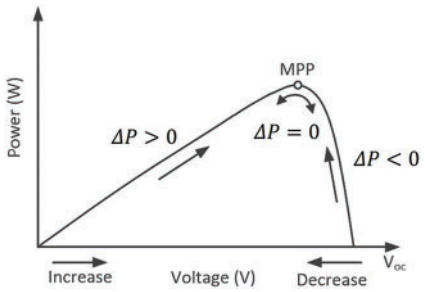

Fig. 7. Conventional P&O MPPT operation strategy.

4.2. *Wind Turbine*

Fig. 6 illustrates the power-speed characteristics of the wind turbine in terms of per unit, providing insight into how its performance varies with different operating conditions.

In this system, the wind turbine is integrated with a permanent magnet synchronous generator (PMSG), a common configuration for wind energy conversion. The operation of the wind turbine is influenced by several factors, including, generator speed, wind speed, and pitch angle. These parameters serve as inputs to the WT block, where calculations are performed to determine the power output. Within the WT block, the power is computed, resulting in torque per unit. This per-unit torque represents the mechanical force exerted by the wind turbine.

The estimated torque generated by the wind turbine is then directed to the PMSG. The PMSG converts the mechanical energy from the turbine into electrical energy, producing three-phase voltages as its output. These voltages are then linked to an AC/DC inverter and a DC/AC inverter.

4.3. *Diesel Generator*

The modeling of a diesel generator system encompasses a diesel engine, excitation system, and synchronous generator. This setup allows the diesel generator to function effectively within the acceptable voltage range of 208 V to 600 V, ensuring stable system operation with consistent fuel input. The diesel generator has a capacity of 455 kW. As a backup system, the diesel generator is initially linked to the breaker before being directly connected to the load.

4.4. *Load*

The system loads operate at 240 volts phase-to-phase. One breaker is also included to simulate load variations encountered in isolated systems.

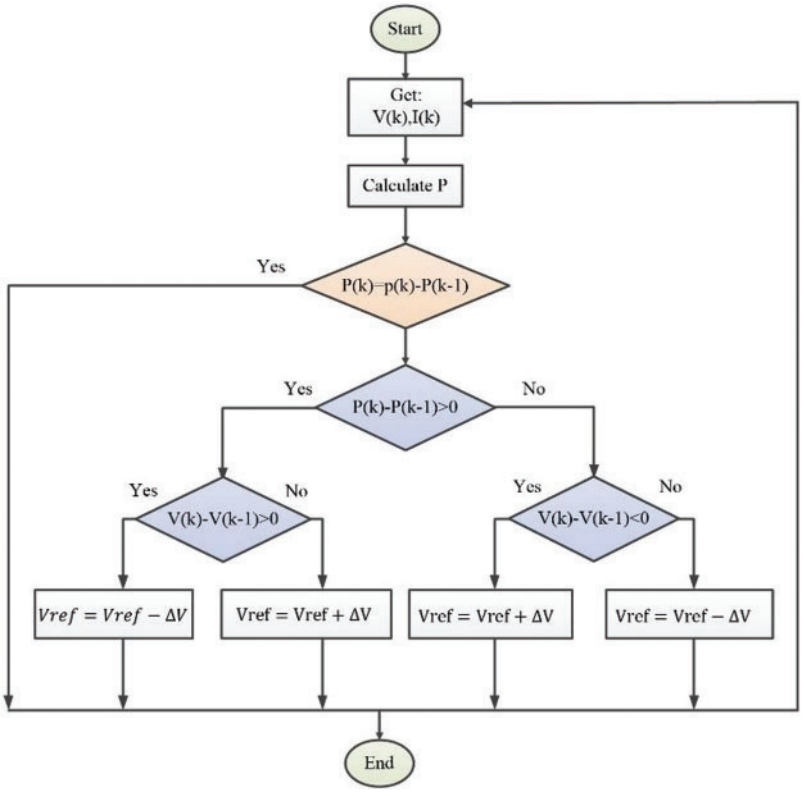

Fig. 8. Flow chart of P&O technique for the MPPT.

5. Control Strategy

5.1. Maximum Power Point Tracking (MPPT)

Solar cell efficiency is affected by multiple factors, including irradiance, temperature, shading, and more. Rapid climate changes, like increased ambient temperature and cloudy weather, can reduce a PV panel's output power [21]. Essentially, each photovoltaic cell's energy production is linked to its operational and environmental conditions. A specific point can be identified on the P-V curve, commonly known as the maximum power point (MPP). This point signifies where the solar cell achieves its highest power output.

Various tracking algorithms have been introduced to optimize the tracking of MPPT in solar PV systems under varying irradiance conditions [22]. The perturbation and observation (P&O) method is a commonly employed approach for MPPT because of its straightforwardness and ease of implementation [23]. The P&O alters the system's operating point, shown in Fig. 7, by introducing incremental voltage changes (ΔV) to the PV array, resulting in a corresponding perturbation of the PV array's output power (ΔP). The P&O persists in introducing voltage disturbances until it reaches the location of the MPP to achieve optimal power extraction from the PV array. The practical algorithm of the MPPT algorithm using the P&O method is shown in Fig. 8.

5.2. Buck Converter

In renewable power systems such as PV, DC-DC converters serve as a method for matching impedances to achieve MPPT, allowing for the optimization of power generation efficiency. These converters play a crucial role in monitoring the system's peak power point by regulating their duty cycle, which consequently adjusts the operating position along the I–V curve.

Among various DC-DC converter topologies, the Buck converter is frequently utilized to reduce the voltage level, ensuring compatibility between the power source and the load. Given that the input voltage from the PV module surpasses the battery terminal's voltage requirement in our case, a buck converter is the ideal choice for our model. The buck converter operates in two distinct phases, beginning with the recharging of the output capacitor when the switch is turned ON. During this phase, the charging current is controlled by the inductor, resulting in a gradual increase in voltage across the capacitor throughout the switching cycle. The designed converter operates at a switching frequency of 10 kHz, featuring an inductance of $L_{Buck} = 0.248\ mH$ and a capacitance of $C_{Buck} = 0.423\ mF$.

6. Simulation Outcome Analysis

To evaluate the performance of dynamic models and controls, various weather conditions are considered, as shown in Table V. A PV system's output voltage, current, and power are shown in Fig. 9. According to Fig. 9, when PV power decreases, PV current output decreases as well, whereas PV voltage remains relatively constant. The MPPT controller manages voltage and current fluctuations to ensure optimal PV output.

Figs. 10 and 11 illustrates state of charge (SOC) and fluctuations in battery voltage, current and output power across various conditions. Changes in battery power is compatible with surplus or insufficient generated power. When load power is lower than the combined output

TABLE V: Weather and Breakers Situations

Time (s)	Irradiance w/m2	Wind speed m/s	DG breaker
0	1000	12	Open
2	600	10	Open
4	200	12	Close
6	400	10	Open
8	600	8	Open

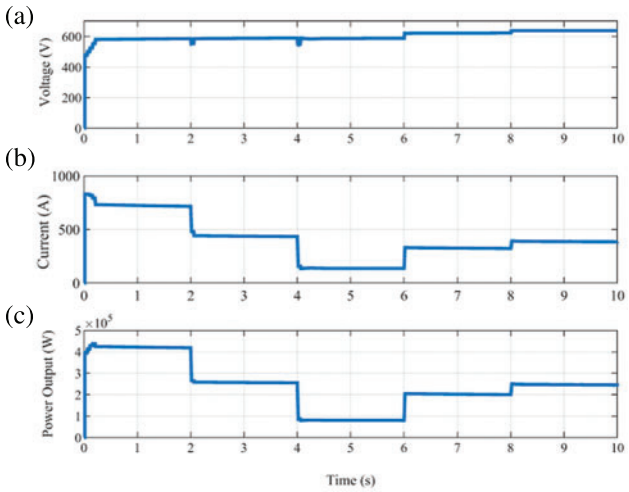

Fig. 9. PV (a) Voltage, (b) Current, and (c) Power for varying solar radiation input.

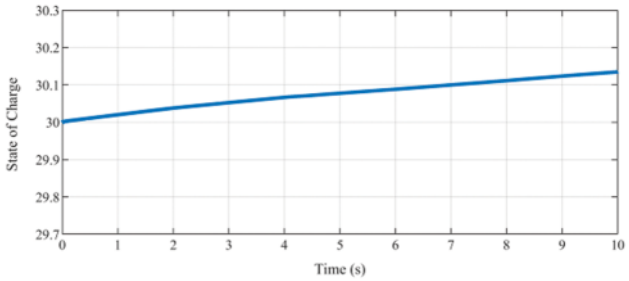

Fig. 10. Battery state of charge.

of WT, PV, and DG, battery output power and current increase, indicating charging. Conversely, when load power exceeds generated power, the battery discharges, leading to a decrease in power and current.

Fig. 12 displays wind turbine output power at different wind speeds. At the base wind speed, the turbine achieves maximum power output, peaking at approximately 500 kW. However, as the wind speed decreases to approximately 10 m/s, the wind power output also diminishes, and again, when wind speed increases, the power increases to its maximum level, which shows that wind power works correctly as well.

The output power of the diesel generator is also shown in Fig. 12. As shown in Fig. 13, the diesel generator provides power when the breakers are closed because it serves as a backup. The diesel generation output remains zero when adequate wind and irradiation exist. The dynamics of the system stabilize approximately 0.15 seconds after it starts operating.

Fig. 14 showcases the output voltage, current, and power load waveforms. The peak load demand in Postville is approximately 400 kW, whereas the average load demand

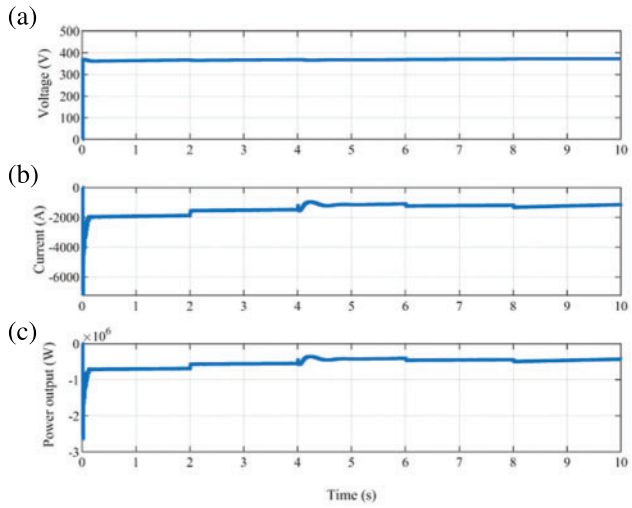

Fig. 11. Battery (a) Voltage, (b) Current, and (c) Power.

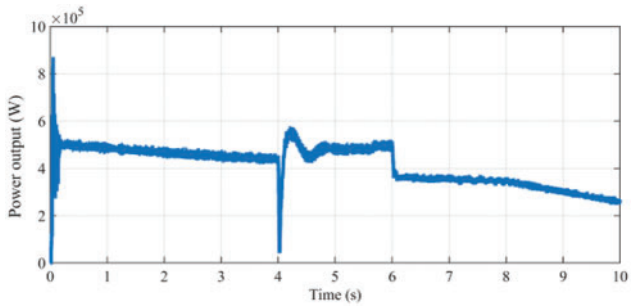

Fig. 12. Wind turbine output power.

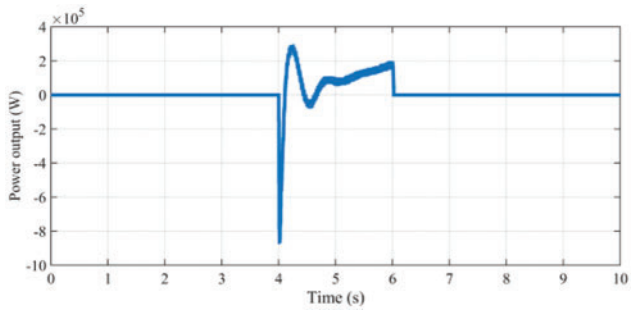

Fig. 13. Diesel generator output power.

is around 200 kW. In this study, the breaker is utilized to represent both the average and peak loads. Initially, the load is 200 kW. Then, between time 4 and 6, the load breaker is closed, adding approximately 200 kW to illustrate the peak load demand accurately. According to Fig. 14, the power output will increase when the breaker is closed, and the voltage peak level will remain constant regardless of the load power.

This setup exemplifies the integration and control of various renewable energy systems including photovoltaic (PV), wind, diesel, and battery systems, along with inverters and converters. The power output of the PV array, WT, and DG align with their designated values. Moreover, the study highlights the effectiveness of MPPT for the PV system, ensuring optimal power generation despite fluctuations in irradiance and temperature.

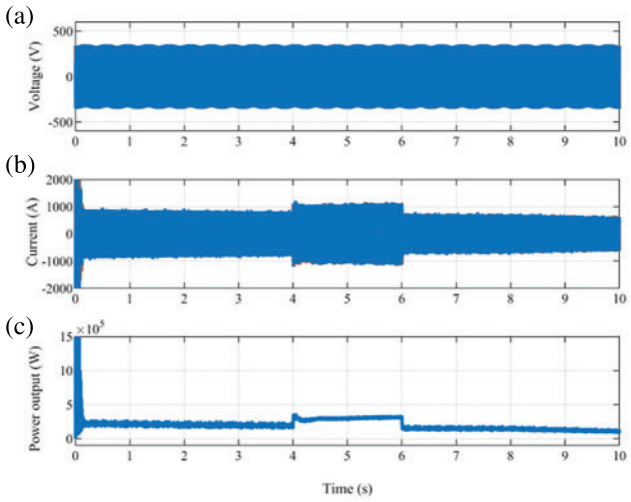

Fig. 14. Load (a) Voltage, (b) Current, and (c) Power.

7. Conclusion

This study proposed a dynamic model for a standalone hybrid power system consisting of PV panels, wind turbines, a diesel generator, and battery storage designed for an isolated community named Postville located in Labrador, Canada. Leveraging MATLAB-Simulink, the system was precisely modeled and simulated, with in-depth discussions on component simulation and control implementation. The simulation results clearly demonstrated the system's reliable performance and viability in meeting the energy needs of Postville.

Conflict of Interest

Authors declare that they do not have any conflict of interest.

References

[1] Mahlia TMI, Saktisahdan TJ, Jannifar A, Hasan MH, Matseelar HS. A review of available methods and development on energy storage; technology update. *Renew Sustain Energ Rev*. 2014 May;33:532–45. doi: 10.1016/j.rser.2014.01.068.

[2] Salisu S, Mustafa MW, Olatomiwa L, Mohammed OO. Assessment of technical and economic feasibility for a hybrid PV-wind-diesel-battery energy system in a remote community of north central Nigeria. *Alex Eng J*. 2019;58(4):1103–18.

[3] Fathy A. A reliable methodology based on mine blast optimization algorithm for optimal sizing of hybrid PV-wind-FC system for a remote area in Egypt. *Renew Energ*. 2016 Sep;95:367–80. doi: 10.1016/j.renene.2016.04.030.

[4] Sun W, Harrison GP. Wind-solar complementarity and effective use of distribution network capacity. *Appl Energy*. 2019 Aug;247:89–101. doi: 10.1016/j.apenergy.2019.04.042.

[5] Al-Ghussain L, Ahmed H, Haneef F. Optimization of hybrid PV-wind system: case study Al-Tafilah cement factory, Jordan. *Sustain Energy Technol Assessments*. 2018 Dec;30:24–36. doi: 10.1016/j.seta.2018.08.008.

[6] Morais H, Kádár P, Faria P, Vale ZA, Khodr HM. Optimal scheduling of a renewable micro-grid in an isolated load area using mixed-integer linear programming. *Renew Energy*. 2010 Jan;35(1):151–6. doi: 10.1016/j.renene.2009.02.03.

[7] Li YS, Bahrami M, Nejad MF, Iqbal MT. Design and simulation of a hybrid power system for St. Lewis in labrador. *European Journal of Electrical Engineering and Computer Science*. 2023;7(1):10–22.

[8] Das S, Akella AK. Power flow control of PV-wind-battery hybrid renewable energy systems for stand-alone application. *Int J Renew Energy Res (IJRER)*. 2018;8:1–43.

[9] Koutroulis E, Kolokotsa D, Potirakis A, Kalaitzakis K. Methodology for optimal sizing of stand-alone photovoltaic/wind-generator systems using genetic algorithms. *Sol Energy*. 2006;80:1072–88.

[10] Belabbas B, Allaoui T, Tadjine M, Denai M. Power management and control strategies for off-grid hybrid power systems with renewable energies and storage. *Energy Syst*. 2019;10:355–84. doi: 10.1007/s12667-017-0251-y.

[11] Ceylan C, Devrim Y. Design and simulation of the PV/PEM fuel cell based hybrid energy system using MATLAB/Simulink for greenhouse application. *Int J Hydrogen Energy*. 2021 Jun;46(42):22092–106. doi: 10.1016/j.ijhydene.2021.04.034.

[12] Farhadi A, Iqbal MT. Optimal sizing and techno-economic analysis of a hybrid power system for postville. *Eur J Eng Technol Res*. 2024 Mar;9(2):5–12. doi: 10.24018/ejeng.2024.9.2.3127.

[13] Hemeida AM, El-Ahmar MH, El-Sayed AM, Hasanien HM, Alkhalaf S, Esmail MFC, *et al.* Optimum design of hybrid wind/PV energy system for remote area. *Ain Shams Eng J*. 2020;11(1):11–23.

[14] Barukčić M, Hederić Ž, Špoljarić Ž. The estimation of I-V curves of PV panel using manufacturers' I-V curves and evolutionary strategy. *Energy Convers Manag*. 2014;88:447–58.

[15] Kotian S, Maliat A, Azeez A, Iqbal T. Design and simulation of a hybrid energy system for Ramea Island, Newfoundland. *2022 IEEE 13th Annual Information Technology, Electronics and Mobile Communication Conference (IEMCON)*. IEEE; 2022.

[16] Martinello D, Carati EG, da Costa JP, Cardoso R, Stein CMO. Emulation of wind turbines. *Wind Turbines-Design, Control and Applications*. 2016;13. doi: 10.5772/63448.

[17] Chong CH, Rigit ARH, Ali I. Wind turbine modelling and simulation using Matlab/SIMULINK. In *IOP Conference Series: Materials Science and Engineering*, vol. 1101, no. 1, IOP Publishing, 2021.

[18] Benhamed S, Ibrahim H, Belmokhtar K, Hosni H, Ilinca A, Rousse D, *et al.* Dynamic modeling of diesel generator based on electrical and mechanical aspects. *2016 IEEE Electrical Power and Energy Conference (EPEC)*. IEEE; 2016.

[19] Charfi S, Atieh A, Chaabene M. Modeling and cost analysis for different PV/battery/diesel operating options driving a load in Tunisia, Jordan and KSA. *Sustain Cities Soc*. 2016;25:49–56.

[20] Achaibou N, Haddadi M, Malek A. Modeling of lead acid batteries in PV systems. *Energy Proc*. 2012;18:538–44.

[21] Shukla A, Khare M, Shukla KN. Modeling and simulation of solar PV module on MATLAB/Simulink. *Int J Innov Res Sci, Eng Technol*. 2015;4(1):18516–27.

[22] Ali AIM, Mohamed HRA. Improved P&O MPPT algorithm with efficient open-circuit voltage estimation for two-stage grid-integrated PV system under realistic solar radiation. *Int J Electr Power Energy Syst*. 2022;137:107805.

[23] Dehghani M, Taghipour M, Gharehpetian GB, Abedi M. Optimized fuzzy controller for MPPT of grid-connected PV systems in rapidly changing atmospheric conditions. *J Mod Power Syst Clean Energy*. 2020;9(2):376–83.